pulse duration is long enough, and comparable to the relaxation time of a multiplet, then relaxation may occur during excitation, which results in an incomplete inversion of the multiplet by the initial selective 180° pulse, and/or in a distortion of the recovery curve obtained by using the 90° monitoring pulse. It is reasonable to believe that if the spin–lattice relaxation times are more than ~ 20–50 times longer than pulse durations, relaxation during the pulses may safely be ignored. However, the relaxation times of the geminal protons of **2** are only eight times longer than the pulse duration used (100 ms), thereby introducing a systematic error into the calculation of their interproton distances.

Conclusion

Various sets of experiments have been used to determine the conformation of the glucosidic bond of **1**. Different selective relaxation experiments gave comparable results, which are in agreement with coupling constant data, whereas nonselective relaxation rates alone failed to give accurate quantitative results because of the limitations discussed, as has been encountered in other relaxation studies of multispin systems. For simpler systems, however (e.g., see ref 11), the nonselective relaxation measurements may be closely consistent with X-ray data.

Acknowledgment. This work was generously supported by the Natural Sciences and Engineering Research Council of Canada, and McGill University. We are especially grateful to George Fainos for writing the computer program used in generating the data of Figure 4. The 400-MHz spectra were recorded at Laboratoire Regional de RMN à Haut Champ, Université de Montréal.

Registry No. 1, 38631-27-5.

300-MHz ^{1}H NMR Study of Parabactin and Its Gallium(III) Chelate

Raymond J. Bergeron* and Steven J. Kline†

Contribution from the Department of Medicinal Chemistry, J. Hillis Miller Health Center, University of Florida, Gainesville, Florida 32610. *Received April 8, 1983*

Abstract: The solution structure of parabactin and its gallium(III) complex is evaluated with 300-MHz ^{1}H NMR. The ligand is shown to exist in three separate conformers while the chelate appears to form the Λ cis chelate exclusively. Furthermore, the chelate is shown to exist in a 3:1 ratio of two diastereomeric forms that differ only in the disposition of the spermidine backbone.

Siderophores are relatively low molecular weight, virtually ferric ion specific ligands. These chelators are produced by microorganisms for the purpose of sequestering exogenous ferric ion and facilitating the transport of this biologically essential metal across the cell membrane.[1,2] The two major classes of siderophores, hydroxamates and catecholamides,[3-7] both from very stable octahedral, high-spin iron(III) complexes with formation constants in excess of 10^{30}. Enterobactin, for example, a cyclic triester of (2,3-dihydroxybenzoyl)serine, is the strongest ferric ion chelating agent known.[8] At pH 7.4, the enterobactin–iron(III) formation constant is 10^{52}. However, much less is known about the spermidine catecholamide siderophore, parabactin (Figure 1), first isolated from an iron-depressed culture of *Paracoccus denitrificans* by Tait in 1975.[9] Since the original isolation of parabactin, most of the studies on this ligand have been focused on the synthesis of this siderophore and its analogues.[10] Little attention has been given to the solution structure of the ligand or its metal complex.

The utilization of a ferric chelate by a microorganism begins with its recognition and transport by membrane receptors. The transport of siderophore metal chelates across microbial cell membranes has been shown in several instances to be stereospecific.[11-13] The recognition of siderophore iron chelates by the microorganism's outer membrane receptors may depend on the configuration of the chelate about the metal center itself, the conformation of various groups in the ligand, or both. As an initial step in a program to evaluate parabactin–receptor interactions, the solution conformation and stereochemistry of parabactin and its gallium chelate was studied.

Experimental Section

General. All reagents, with the exception of L-(*tert*-butoxycarbonyl)threonine (Sigma Chemical) and gallium(III) nitrate-9H_2O (Alfa) were purchased from Aldrich Chemical Co. and were used without further purification. Na_2SO_4 was used as a drying agent. Melting points were taken on a Fisher–Johns apparatus and are uncorrected. Preparative thin-layer chromatography was done on 20 × 20 cm silica gel plates obtained from Analtech. Sephadex LH-20 was purchased from Pharmacia Fine Chemicals. Optical rotations were measured with a Perkin-Elmer Model 141 polarimeter. Elemental analyses were performed by Galbraith Laboratories, Knoxville, TN, or Atlantic Microlab Inc., Atlanta, GA. Proton NMR spectra were obtained on a Nicolet Instrument Corp. NT-300 spectrometer and NIC-1180 E data system. Probe temperature was determined with test samples of ethylene glycol. Computer simulation and curve analysis/deconvolution programs used were included in the NMCFT software package provided by Nicolet Technology Corp. Resolution enhancement, when necessary, was performed by apodization of the FID by a double-exponential multiplication followed by zero filling. Samples for the determination of temperature of coalescence were prepared by dissolving 5–10 mg of the compound in 500 μL of Me_2SO-d_6. Coalescence temperatures, ±1 °C, were then deter-

† Current address: Abbott Laboratories, Abbott Park, IL 60064.

(1) Neilands, J. B. In "Microbial Iron Metabolism"; Neilands, J. B., Ed.; Academic Press: New York, 1974; pp 3–34.
(2) Emery, T. In "Metal Ions in Biological Systems"; Sigel, H., Ed.; Marcel Dekker: New York, 1978; Vol. 7, pp 77–125.
(3) Neilands, J. B. *Ann. Rev. Biochem.* **1981**, *50*, 715–731.
(4) Raymond, K. N.; Carrano, C. J. *Acc. Chem. Res.* **1979**, 183–190.
(5) Neilands, J. B. *Ann. Rev. Nutr.* **1981**, *1*, 27–46.
(6) Raymond, K. N. *Adv. Chem. Ser.* **1977**, *162*, 33–54.
(7) Neilands, J. B.; Peterson, T.; Leong, S. A. In "Inorganic Chemistry in Biology and Medicine"; Martell, A. E., Ed.; American Chemical Society: Washington, DC, 1980; pp 263–278.
(8) Harris, W. R.; Carrano, C. J.; Raymond, K. N. *J. Am. Chem. Soc.* **1979**, 101, 2213–2214.
(9) Tait, G. H. *Biochem. J.* **1975**, *146*, 191–204.
(10) Bergeron, R. J.; Kline, S. J. *J. Am. Chem. Soc.* **1982**, *104*, 4489–4492.
(11) Winkelmann, G. *FEBS Lett.* **1979**, *97*, 43–46.
(12) Neilands, J. B.; Erickson, T. J.; and Rastettler, W. H. *J. Biol. Chem.* **1981**, *265*, 3831–3832.
(13) Winkelmann, G.; Braun, V. *FEMS Microbiol. Lett.* **1981**, *11*, 237–241.

0002-7863/84/1506-3089$01.50/0 © 1984 American Chemical Society

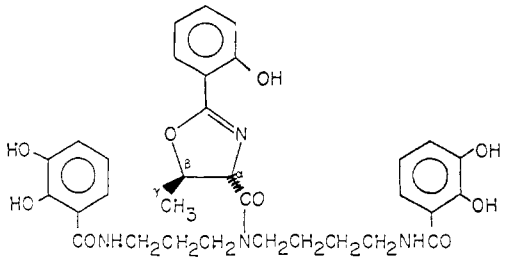

Figure 1. Parabactin.

mined by observing the coalescence of the β-decoupled γ-methyl signals. The coalescence temperatures were measured both on heating and cooling cycles and activation energies, ±0.2 kcal/mol, subsequently calculated by the method of Gutowsky and Cheng.[14] Chemical shifts are reported downfield from an external DSS standard. Me_2SO-d_6/$CDCl_3$ titrations were carried out by dissolving a sample of 5 mg of parabactin in 500 μL of $CDCl_3$ in a 5 mm o.d. NMR tube. Additions of Me_2SO-d_6 were made directly into the NMR tube via a microliter syringe and spectra recorded after mixing the sample. In this manner spectra were recorded at Me_2SO-d_6 concentrations (volume percent) of 0%, 2%, 5%, 20%, 30%, 40%, and 50%. pH measurements were obtained with an Ingold microelectrode. Gallium chelates were prepared by adding a slight excess of $Ga(NO_3)_3$ to an aqueous solution of the catecholamide at ~pH 10 and immediately adjusting the pH to ~7.4 under N_2. Water was removed in vacuo after allowing the mixture to stir overnight at room temperature.

L-*N*-Hydroxysuccinimido *N*-(*tert*-Butoxycarbonyl)threoninate (1). Dicyclohexylcarbodiimide (DCC) (2.97 g, 14.4 mmol) in THF (100 ml) was added to a solution of L-*N*-(*tert*-butoxycarbonyl)threonine (2.96 g, 13.5 mol) and *N*-hydroxysuccinimide (1.63 g, 14.2 mmol) in dry THF (100 mL) at 0 °C. The mixture was allowed to warm slowly to room temperature with continued stirring under N_2. After 14 h, the mixture was filtered and the DCU washed with THF (25 mL). The solvent was evaporated and the residue crystallized from diethyl ether to yield 3.84 g (90%) of **1** as white crystals: mp 134–135 °C, $[\alpha]^{24}_D$ −33.7 ±0.7 (*c* 2.7, EtOAc) (lit. mp 134–135 °C, $[\alpha]^{25}_D$ −33.3 (EtOAc));[15] ^{1}H NMR ($CDCl_3$) δ 1.25 (d, 3 H), 1.47 (s, 9 H), 2.78 (s, 4 H), 3.89–4.98 (m, 3 H), 6.38 (m, 1 H).

L-N^4-[*N*-(*tert*-Butoxycarbonyl)threonyl]-N^1,N^8-bis(2,3-dimethoxybenzoyl)spermidine (2). A solution of N^1,N^8-bis(2,3-dimethoxybenzoyl)spermidine[16] (2.50 g, 5.28 mmol) in DMF (150 mL) was cooled to 0 °C. A solution of **1** (1.75 g, 5.54 mmol) in DMF (50 mL) was added at once and the mixture allowed to warm slowly to room temperature. After 48 h the solvent was evaporated. The residue was dissolved in CH_2Cl_2 (100 mL), washed with cold 3% (w/v) aqueous HCl (3 × 30 mL) and cold water (10 × 30 mL), dried, filtered, and evaporated. Silica gel chromatography (5% MeOH/EtOAc) yielded **2** as a hygroscopic white solid: 2.99 g (84%); ^{1}H NMR ($CDCl_3$) δ 1.13 (d, 3 H), 1.40 (s, 9 H), 1.50–2.13 (m, 6 H partially obscured), 3.07–3.63 (m, 8 H), 3.83 (s, 12 H), 4.17–4.57 (m, 3 H), 5.33–5.60 (d, 1 H), 6.77–8.27 (m, 8 H).

Anal. Calcd for $C_{34}H_{50}N_4O_{10}$: C, 60.52; H, 7.47; N, 8.30. Found: C, 60.60; H, 7.38; N, 8.45.

L-N^4-Threonyl-N^1,N^8-bis(2,3-dimethoxybenzoyl)spermidine (3). A solution of **2** (1.70 g, 0.25 mmol) in TFA (40 mL) was stirred at room temperature for 45 min. The solvent was then evaporated and the residue dissolved in cold CH_2Cl_2 (100 mL), washed with ice-cold 30% (w/v) aqueous sodium carbonate (3 × 50 mL), dried, filtered, and evaporated. Purification on silica gel (10% MeOH/$CHCl_3$) provided 1.38 g (95%) of **3** as a hygroscopic white solid. ^{1}H NMR ($CDCl_3$) δ 1.10–1.20 (d, 3 H), 1.43–2.00 (m, 6 H), 2.94–4.08 (overlapping, 25 H), 6.84–8.25 (m, 8 H).

Anal. Calcd for $C_{29}H_{42}N_4O_8$: C, 60.61; H, 7.37; N, 9.75. Found: C, 60.50; H, 7.36; N, 9.62.

L-N^4-Threonyl-N^1,N^8-bis(2,3-dihydroxybenzoyl)spermidine Hydrobromide (4). To a 1 M stirred solution of BBr_3 (20 mL, 20.0 mmol) in dry CH_2Cl_2 (30 mL) at 0 °C was added **3** (0.83 g, 1.44 mmol) in CH_2Cl_2 (30 mL) dropwise under N_2. The reaction mixture was allowed to warm slowly to room temperature. After 12 h, the reaction vessel was cooled to 0 °C, and ice-cold water (15 mL) was added dropwise with vigorous stirring. The resulting suspension was allowed to warm to room temperature with continued stirring over 1 h and the product collected by filtration. The residue was dissolved in MeOH and evaporated; this process was repeated several times. Chromatography on Sephadex LH-20 (20% → 40% EtOH/benzene) gave 0.78 g (90%) of **4** as a white solid. ^{1}H NMR (CD_3OD) δ 1.10–1.37 (d, 3 H), 1.43–2.23 (m, 6 H), 3.13–3.80 (m, 8 H), 3.83–4.40 (m, 3 H), 6.33–7.33 (m, 6 H).

Anal. Calcd for $C_{25}H_{35}N_4O_8Br$: C, 50.09; H, 5.88; N, 9.35. Found: C, 49.98; H, 5.96; N, 9.27.

L-*N*-[3-(2,3-Dihydroxybenzamido)propyl]-*N*-[4-(2,3-dihydroxybenzamido)butyl]-2-(2-hydroxyphenyl)-*trans*-5-methyloxazoline-4-carboxamide (Parabactin) (5). A solution of **4** (0.35 g, 0.59 mmol) and ethyl 2-hydroxybenzimidate[17] (0.11 g, 0.67 mmol) in dry MeOH (50 ml) was heated to reflux. After 24 h the solvent was evaporated and the residue chromatographed on Sephadex LH-20 (20% EtOH/benzene) providing 0.31 g (85%) of **4** as a white solid $[\alpha]^{25}_D$ 98 ± 2° (c 3.0, methanol). ^{1}H NMR (10:1, $CDCl_3$/Me_2SO-d_6) δ 1.34–1.45 (m, 3 H), 1.48–2.03 (m, 6 H), 3.11–3.78 (m, 8 H), 4.59 (m, 1 H), 5.28–5.45 (m, 1 H), 6.52–7.71 (m, 10 H), 7.89–8.17 (m, 4 H), 11.56–12.82 (m, 3 H).[18]

Anal. Calcd for $C_{32}H_{36}N_4O_9$: C, 61.93; H, 5.85; N, 9.03. Found: C, 61.93; H, 5.94; N, 8.96.

L-*N*-[3-(2,3-Dimethoxybenzamido)propyl]-*N*-[4-(2,3-dimethoxybenzamido)butyl]-2-(2-hydroxyphenyl)-*trans*-5-methyloxazoline-4-carboxamide (6). A solution of **3** (0.49 g, 0.85 mmol) and ethyl 2-hydroxybenzimidate (0.148 g, 0.86 mmol) in dry MeOH (25 mL) was heated to reflux under N_2. After 24 h the solvent was evaporated and the residue was dissolved in CH_2Cl_2 (50 mL) and washed with cold H_2O (2 × 25 mL). The organic phase was dried, filtered, and evaporated. Purification on silica gel (10% MeOH/$CHCl_3$) provided 0.48 g (83%) of **4** as a white, hygroscopic solid. ^{1}H NMR (10:1, $CDCl_3$/Me_2SO-d_6) δ 1.44–1.53 (m, 3 H), 1.56–2.13 (m, 7 H), 3.53–3.63 (m, 8 H), 3.84–3.96 (m, 12 H), 4.62–4.70 (m, 1 H), 5.17–5.48 (m, 1 H), 6.83–7.68 (m, 10 H), 7.98–8.38 (m, 2 H), 11.56 (s, 1 H).

Anal. Calcd for $C_{36}H_{44}N_4O_9$: C, 63.89; H, 6.55; N, 8.28. Found: C, 63.75; H, 6.78; N, 8.19.

L-N^5-[*N*-(*tert*-Butoxycarbonyl)threonyl]-N^1,N^9-bis(2,3-dimethoxybenzoyl)homosperimidine (7) was prepared and purified in the same manner as **2**: 82% yield; ^{1}H NMR ($CDCl_3$) δ 1.14 (d, 3 H), 1.40 (s, 9 H), 1.48–2.14 (m, 8 H partially obscured), 3.05–3.64 (m, 8 H), 3.82 (s, 12 H), 4.15–4.55 (m, 3 H), 5.31–5.60 (d, 1 H), 6.77–8.26 (m, 8 H).

Anal. Calcd for $C_{35}H_{52}O_{10}$: C, 61.03; H, 7.61; N, 8.13. Found: C, 61.12; H, 7.83; N, 7.98.

L-N^5-Threonyl-N^1,N^9-bis(2,3-dimethoxybenzoyl)homospermidine (8) was prepared and purified in the same manner as **3**: 95% yield; ^{1}H NMR ($CDCl_3$) δ 1.09–1.20 (d, 3 H), 1.44–1.99 (m, 8 H), 2.95–4.00 (overlapping, 25 H) 6.84–8.25 (m, 8 H).

Anal. Calcd for $C_{30}H_{44}N_4O_8$: C, 61.21; H, 7.53; N, 9.52. Found: C, 61.10; H, 7.41; N, 9.30.

L-N^5-Threonyl-N^1,N^9-bis(2,3-dihydroxybenzoyl)homospermidine hydrobromide (9) was prepared and purified in the same manner as **4**: 88% yeild; ^{1}H NMR (CD_3OD) δ 1.11–1.40 (d, 3 H), 1.40–2.24 (m, 8 H), 3.10–3.83 (m, 8 H), 3.83–4.40 (m, 3 H), 6.34–7.41 (m, 6 H).

Anal. Calcd for $C_{26}H_{37}N_4O_8$·Br: C, 50.90; H, 6.08; N, 9.13. Found: C, 51.01; H, 5.95; N, 9.31.

L-*N*-[4-(2,3-Dihydroxybenzamido)butyl]-*N*-[4-(2,3-dihydroxybenzamido)butyl]-2-(2-hydroxyphenyl)-*trans*-5-methyloxazoline-4-carboxamide (homoparabactin) (10) was prepared and purified in the same manner as **5**: 82% yield; ^{1}H NMR (10:1, $CDCl_3$/Me_2SO-d_6) δ 1.30–1.44 (m, 3 H), 1.50–2.02 (m, 8 H), 3.10–3.77 (m, 8 H), 4.61 (m, 1 H), 5.30–5.45 (m, 1 H), 6.52–7.70 (m, 10 H), 7.89–8.17 (m, 4 H), 11.55–12.82 (m, 3 H).

Anal. Calcd for $C_{33}H_{38}N_4O_9$: C, 62.45; H, 6.04; N, 8.83. Found: C, 62.53; H, 5.94; N, 8.93.

Synthesis

The synthesis is essentially as reported earlier,[10] with one exception. The *N*-*tert*-butoxycarbonyl protecting group of the threonine moiety was used instead of the *N*-carbobenzoxy protecting group. The *tert*-butoxycarbonyl protecting group was chosen because of the ease with which it can be removed. Briefly, the synthesis begins with the acylation of N^1,N^8-bis(2,3-dimethoxybenzoyl)spermidine with the *N*-hydroxysuccinimidyl ester of L-*tert*-butoxycarbonyl)threonine to form the condensation product **2** in 84% yield after purification on silica gel. The *tert*-butoxy protecting group is next removed with TFA, and after purification on silica gel, **3** is obtained in 95% yield. Boron tribromide in

(14) Gutowsky, H. S., Cheng, H. N. *J. Chem. Phys.* **1975**, *63*, 2439–2441.
(15) Storey, H. T.; Beacham, J.; Cernosek, S. F.; Finn, F. M.; Yanaihara, C.; Hofmann, K. *J. Am. Chem. Soc.* **1972**, *94*, 6170–6178.
(16) Bergeron, R. J.; Kline, S. J.; Stolowich, N. J.; McGovern, K. A.; Burton, P. S. *J. Org. Chem.* **1981**, *46*, 4524–4529.
(17) Easson, A. P. T., Pyman, F. L. *J. Chem. Soc.* **1931**, 2991.
(18) The ^{1}H NMR spectrum of a sample of parabactin isolated from *Paracoccus denitrificans* was found to be essentially identical with the spectrum of synthetic parabactin. The authors thank J. B. Neilands for supplying the isolated sample of parabactin.

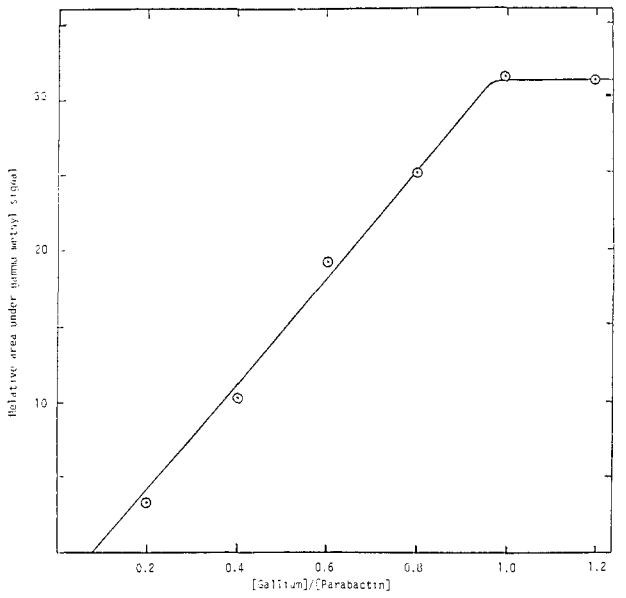

Figure 2. Titration of parabactin with gallium(III) in D_2O: integration of the γ-methyl signal vs. the [gallium]/[parabactin] molar ratios.

methylene chloride is next used to demethylate **3**. The hydrobromide of the resulting catecholamide is purified on Sephadex LH-20, providing **4** in a 90% yield. The final cyclization of **4** with 2-hydroxybenzimidate proceeds smoothly, and after purification on Sephadex LH-20, parabactin is obtained in 84% yield.

The tetramethylated derivative of parabactin **6** was prepared in 83% yield by condensing **3** with (2-hydroxybenzimino)ethyl ether. Finally, the above synthesis was applied to the synthesis of homoparabactin by beginning with N^5-benzylhomospermidine.

Results

Stoichiometry of Chelate. The stoichiometry of the parabactin–gallium chelate was determined by titrating a basic solution of parabactin in D_2O with $Ga(NO_3)_3 \cdot 9H_2O$ in D_2O and observing the increase in integrated intensity of the γ-methyl signal of the resulting complex. Figure 2 shows a plot of the integrated intensity of the γ-methyl signal of the parabactin–gallium complex against the [gallium]/[parabactin] ratio. The break in the linear plot at a [gallium]/[parabactin] ratio of 1.0 is consistent with parabactin forming a 1:1 complex with gallium.

Amide protons. In Me_2SO-d_6 four distinct amide NH resonances are observable for the parabactin–gallium chelate, Figure 3ab, a set of large peaks centered at 11.04 and 10.78 ppm and a smaller pair of signals at 11.11 and 10.33 ppm. The two peaks comprising each set integrate equally, while a comparison of the total integrated area between the two sets reveals a 3:1 ratio. All four of these amide NH resonances consist of a set of fairly well-resolved doublet of doublets, each multiplet arising from separate splitting by the two geminal protons on adjacent carbon atoms. By irradiating the appropriate individual methylene protons, the coupling constants for each amide signal were obtained, Table I. Finally, the temperature dependence of the four amide NH proton chemical shifts was examined in Me_2SO-d_6, and the slopes of the linear chemical shift vs. temperature plot for each amide NH is summarized in Table I.

Unlike the ^1H NMR spectrum of the parabactin–gallium complex in Me_2SO-d_6 where four distinct amide NH signals were observed, the spectrum of the chelate in D_2O revealed only a single amide proton. This single amide NH resonance is a well-resolved doublet of doublets corresponding to an AMX spin system with $J_{ax} = 8.4$ and $J_{mx} = 4.3$ Hz. Like the amide protons observed in Me_2SO-d_6, this signal occurs at an unusually low field for amide protons, 10.62 ppm. Integration of this multiplet shortly after preparation of the sample indicated only 0.7 proton. The signal completely disappears after 2–3 days in D_2O.

Oxazoline Ring Protons: α, β, and γ Protons. The γ-methyl protons of the parabactin gallium chelate in D_2O at 22 °C appear

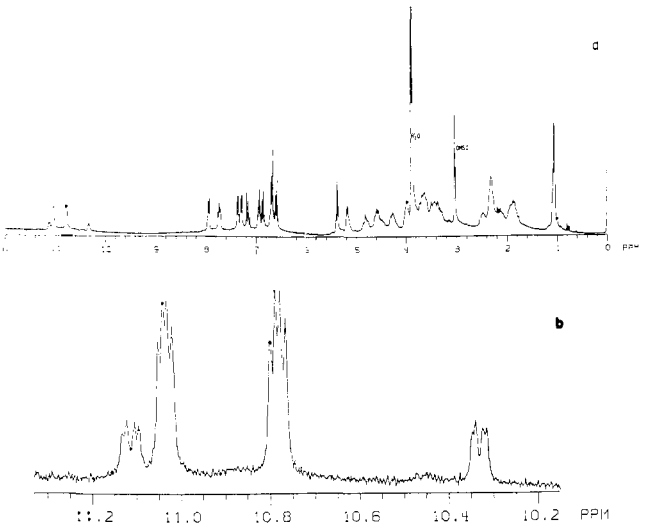

Figure 3. (a) 300-MHz ^1H NMR spectrum of the parabactin–gallium(III) chelate in Me_2SO-d_6. (b) The four amide NH signals of the parabactin–gallium(III) chelate.

Table I. Amide NH Proton Data for the Parabactin–Gallium(III) Chelate

NMR solvent	chemical shift, ppm	slope of plot of chemical shift vs. temperature, (ppm/°C)10^3	coupling constants, Hz
	11.11	0.80	3.9, 8.3
DMe_2SO-d_6	11.04	0.37	3.7, 6.7
	10.78	0.22	3.8, 7.1
	10.33	0.18	3.2, 7.8
D_2O	10.62	not measured	4.3, 8.4

as a sharp doublet centered at 0.62 ppm with a $J_{\gamma,\beta}$ of 6.2 Hz. The α- and β-methine signals occur at similar chemical shifts and are almost completely obscured by the HOD peak. However, on heating the sample to 30 °C, the HOD resonance moves upfield revealing a complex multiplet centered at 4.79 ppm. This multiplet is simplified into two overlapping AB doublets when the γ-methyl peak is decoupled. A computer simulation was utilized to extract the chemical shifts and coupling constants of the A and B members comprising the two AB doublets. It was thus determined that the chemical shift of the α-methylene proton is 4.82 ppm in the minor set and 4.80 ppm in the major set of doublets. Likewise, the chemical shift of the β-methine proton was determined to be 4.78 and 4.76 ppm, for the minor and major sets, respectively, while $J_{\alpha,\beta}$ is 2.5 Hz for both sets of AB doublets.

The parabactin gallium chelate's ^1H NMR spectrum in Me_2SO-d_6 reveals the γ-methyl group as a pair of partially overlapping doublets (Figure 3). Decoupling the β-methine resonance afforded the chemical shift values of 1.05 and 1.09 ppm for the minor and major γ-methyl signals, respectively, while computer simulation provided the coupling constant $J_{\gamma,\beta} = 6.4$ Hz for both doublets. At 22 °C in Me_2SO-d_6 the α-methine appears as a pair of doublets. The minor doublet is located at 5.40 ppm with $J_{\alpha,\beta} = 2.3$ Hz, while the major doublet is found slightly upfield at 5.37 ppm with the same $J_{\alpha,\beta}$ as the minor doublet. The β-methine proton emerges as a complex multiplet, which is simplified into two doublets upon irradiation of the γ-methyl resonance. The chemical shift of these two doublets is 5.22 and 5.19 ppm, corresponding to the minor and major sets, respectively.

External Methylene Protons. The signal falling in the region between 3.0 and 4.4 ppm in the ^1H NMR spectrum of the parabactin–gallium chelate in D_2O are assigned to those eight methylene protons of the spermidine chain that are adjacent to nitrogen, protons on C(1), C(3), C(5), and C(8). Examination of the signals in this area reveals several well-resolved multiplets (Figure 4). The nonequivalence of the geminal methylene protons is very clear. There is enough separation between the signals such

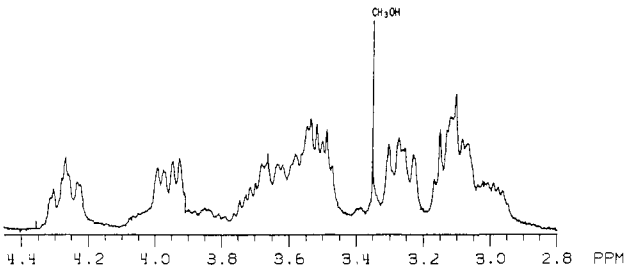

Figure 4. External methylene region of the parabactin–gallium chelate in D_2O after all NH protons have been exchanged with D_2O. Double-resonance difference spectra generated by subtraction of spectra obtained during irradiation of individual external methylene protons from spectra in which the decoupling frequency was set off resonance.

that double resonance experiments provides assignment of this region complete with geminal and vicinal coupling constants. Irradiation of the lone amide NH signal in D_2O lead to a partial collapse of the multiplets at 3.96 and 3.27 ppm. These two peaks can therefore be assigned to the methylene protons on one of the terminal methylene carbons C(1) or C(8); however, differentiation between the two possibilities cannot be made from these data alone. In the spectrum of the gallium chelate in which all amide protons have been completely replaced with deuterons, the peaks at 3.96 and 3.27 ppm appear as two apparent quartets, each proton split once by its nonequivalent geminal proton and again by one of the two vicinal protons on the adjacent carbon. Irradiation of the apparent quartet at 3.96 ppm reduced the multiplet at 3.27 ppm into a doublet with a J_{vic} of 8.8 Hz. Decoupling the peak at 3.27 ppm reduced the signal of 3.96 ppm to a doublet with J_{vic} of 5.7 Hz. Decoupling the multiplet at 4.26 ppm produced a simplification of the overlapping resonance at 3.09 ppm. This second pair of geminal protons were found to be separated by 360 Hz. This irradiation provided a single vicinal coupling constant of 4.4 Hz for the upfield portion of the overlapping peaks at 3.09 ppm. Decoupling the region at 3.09 ppm reduced the multiplet at 4.26 ppm into a doublet of doublets, corresponding to vicinal coupling constants of 3.4 and 10.5 Hz. A third set of geminal methylene protons was discovered by irradiating the upfield portion of the overlapping set of peaks corresponding to three protons at 3.6 ppm, reducing the downfield side of the resonance at 3.1 ppm, into an apparent triplet. The apparent triplet was really two doublets of equal vicinal coupling constant of 5.5 Hz. Due to the extensive overlapping of the resonances in the 3.6 ppm region, no further information regarding vicinal coupling constants would be obtained. However, process of elimination dictates the two remaining geminal methylene protons yet to be assigned must lie in the downfield portion of this overlapping region.

Close examination of the multiplets comprising the external methylene proton region reveals the presence of a second, smaller set of methylene signals. Such duplicity of proton resonances in the spectrum of the parabactin–gallium chelate has been encountered in all previous spectral regions described so far; however, the presence of such additional signals, presumably arising from a second parabactin–chelate species, is not quite so obvious in this region of the ^1H NMR spectrum. Inspection of this spectral region (Figure 4) indicates the second set of signals are not really duplications of the major set of multiplets simply shifted to a lower or higher field, although a rough chemical shift correlation between individual minor and major multiplets does appear to exist. No quantitative assignment involving correlation of minor or major signals was undertaken due to the poor resolution of these signals. In fact, even the most qualitative analysis of the multiplicity in the smaller set of signals was precluded due to the general lack of resolution in the smaller multiplets and their partial overlap with the major external protons' resonances. However, an integration of the multiplets comprising this region demonstrates the presence of a second chelate species quite clearly. The integration of the multiplets in this region is summarized along with chemical shifts for both major and minor species in Table II. An extensive study of the smaller set of external proton multiplets, although

Table II. "External" Methylene Proton Data for the Parabactin-Gallium(III) Chelate

chemical shift, ppm	integration, protons	vicinal coupling constants, Hz
4.26	0.7	10.5, 3.4
4.05	0.15	*a*
3.96	0.7	5.7
3.84	0.3	*a*
3.45-3.75	2.6	*a*
3.27	1.1	8.8
3.14, 3.09	1.7	5.5, 4.4
2.99	0.8	*a*

[a] Unable to measure.

Table III. Double-Resonance Difference Spectral Data for the Parabactin-Gallium(III) Chelate in D_2O

f_2, ppm	ppm of perturbation in resultant difference spectra		
4.26	2.03		
3.96	1.98		
3.67	2.11		
3.55		1.77	1.63
3.27	2.03		
3.11	1.98	1.74	1.63

desirable, was not critical to our evaluation of the parabactin–gallium chelate's solution conformation since a large amount of information still could be obtained by studying the major set of resonances.

Internal Methylenes and Double-Resonance Difference Spectroscopy. In D_2O, protons on the internal carbons of the spermidine chain, specifically C(2), C(6), and C(7), fall in a region between 2.2 and 1.6 ppm, which integrates out to six protons. Although the complexity of overlapping peaks in this region rendered analysis by conventional double-resonance experiments all but useless, considerable information was gained from the difference spectra obtained by irradiation of external methylene proton multiplets. Double-resonance difference spectroscopy[19,20] was utilized to obtain the approximate chemical shifts for the six overlapping internal methylene protons. Difference spectra were generated by subtraction of the spectra obtained during irradiation of individual external methylene protons from spectra in which the decoupling frequency was set off resonance. In this way, resonances of all internal methylene protons not coupled to the irradiated external methylene proton will cancel out in the spectrum subtraction. Coupling between an internal methylene proton and the irradiated external methylene proton will be indicated by the presence of a large perturbation in the difference spectrum. The center of these perturbations represents the chemical shift of the internal methylene proton coupled to the irradiated external methylene proton. Thus, from the major perturbations in the difference spectra, approximate chemical shifts were elucidated for all six internal methylene protons and are listed in Table III. An example of the technique is shown in Figure 5 where irradiation of the external proton multiplet at 4.26 ppm leads to a single major perturbation in the difference spectrum centered at 2.03 ppm. This indicates the external methylene proton at 4.26 ppm is coupled to the internal methylene proton at 2.03 ppm.

Although exact chemical shift values cannot be elucidated, it is still possible to determine by inspection if two perturbations in the difference spectra occur at different frequencies. For example, Figure 5 shows that although one might have difficulty in determining the center of the perturbations in spectra f and g, it is clear that the two perturbations do occur at two different frequencies.

(19) Kuo, M. C.; Gibbons, W. A. *Biochemistry* **1979**, *18*, 5855–5867.
(20) Wyssbrod, H. R.; Fischman, A. J.; Wittbold, W. M.; Smith, C. W.; Walter, R.; Schwartz, I. L. *Int. J. Pept. Protein Res.* **1981**, *17*, 48–55.

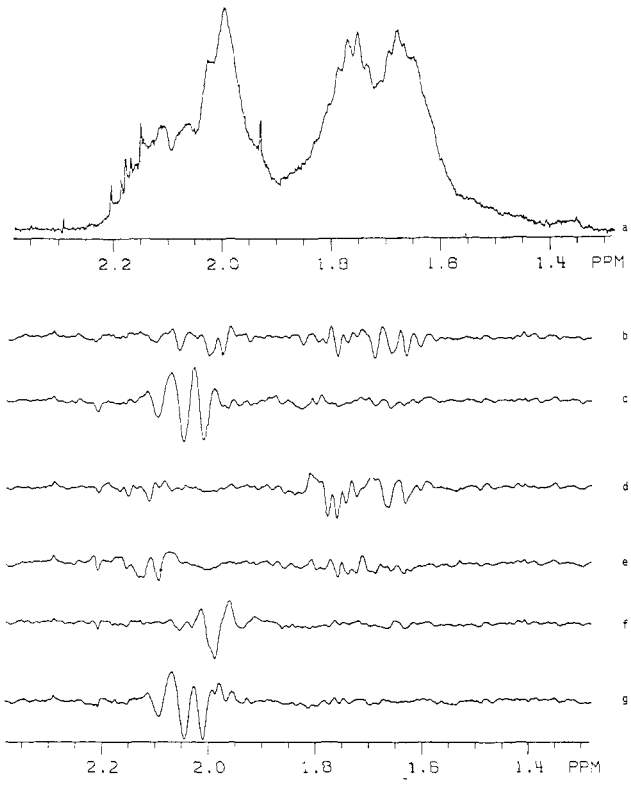

Figure 5.

Discussion

Conformational Isomerism of the Free Ligand. Earlier, we reported that parabactin's ^{1}H NMR spectrum showed three sets of γ-methyl doublets in 10:1 $CDCl_3/Me_2SO$-d_6 at 23 °C.[10] The α-methine multiplet in this solvent is characterized by five lines at 23 °C, which increase to six lines, three sets of doublets, upon cooling to −13 °C. The α-methine multiplet in Me_2SO-d_6 revealed five lines at 23 °C, presumably three sets of doublets with two of the doublets partially overlapping. It appears that parabactin exists in at least three different isomeric species in the solvents examined.

Although the included data cannot define the exact nature of this isomerism, certain deductions can be made concerning its origin. All three of the isomers exhibit α,β coupling constants of approximately 6.8 Hz consistent with trans coupling. Therefore, the possibility that one of the isomers is a *cis*-oxazoline ring is unlikely.[21,22] It is equally unlikely that one of the three isomers is the product of oxazoline ring hydrolysis resulting in an open form of parabactin due to the well-established differences in chemical shifts and coupling constants of the α, β, and γ protons in the open and closed forms of the siderophore.[22] The evidence clearly suggests that the siderophore exists as three different, interconverting conformers.[22,23] Two suggestions as to the origin of the conformational isomerism resulting in at least two major solution conformers involve (1) an approximate 180° rotation about the N^4-carbonyl carbon–α-carbon[23] bond and (2) ~180° rotation about the N^4-carbonyl carbon tertiary amide bond in a classical cis–trans amide bond isomerism.[22] The importance of (2) in controlling conformer populations is underscored by the observation that homoparabactin lacks the duplicity in ^{1}H NMR signals observed for parabactin.

An attempt was made to evaluate the various intramolecular interactions responsible for establishing the energy barrier that must be overcome for interconversion between the conformers. As previously noted, the ^{1}H NMR spectrum of parabactin is extremely sensitive to the particular solvent used. Changes in both chemical shift and conformer population occur upon relatively small change in the solvent. This situation is typified by the addition of small amounts of Me_2SO-d_6 to a $CDCl_3$ solution of parabactin. Two sets of γ-methyl signals exist in approximately a 7:1 ratio in $CDCl_3$. Addition of small amounts of Me_2SO-d_6 to the sample results in a steady decrease in this ratio until the spectrum of parabactin in neat Me_2SO-d_6 shows the γ-methyl peaks in an approximate 1:1 ratio. Such a solvent dependency on conformer population suggests that intramolecular hydrogen bonding plays a role in determining the interconversion between conformational isomers. Since $CDCl_3$ has relatively poor hydrogen bond donor and acceptor abilities, a large degree of intramolecular hydrogen bonding could be expected to occur in $CDCl_3$ solutions of the siderophore; thus, the conformer population in this solvent would be largely influenced by intramolecular hydrogen bonds. The addition of a good hydrogen bond acceptor, Me_2SO, would compete for hydrogen bond donor sites, leading to a disruption of intramolecular hydrogen bonding. The disruption of the weaker intramolecular hydrogen bonds by Me_2SO-d_6 could explain the change in conformer population observed during the titration.

The magnitude of the internal rotational energy barrier that must be overcome for interconversion between the conformers of parabactin was determined by measuring the coalescence temperature, T_c, of the two γ-methyl signals in Me_2SO-d_6. Thus, the energy of activation (E_a) for the interconversion between conformers can be calculated by the method of Gutowsky and Cheng.[14] Any intramolecular hydrogen bonding present will result in an increase in this energy barrier since interconversion between conformers is likely to require the breaking of some of these bonds. To elucidate the contribution to the rotational energy barrier by the hydrogen bond donating ability of the catechol groups, a tetramethylated derivative of parabactin was synthesized and its T_c measured. Methylation of the catechols will eliminate hydrogen bond donation by these groups. As expected, elimination of the hydrogen bonding component to the internal rotational barrier resulting from hydrogen bonding by catechol groups resulted in a markedly lower coalescence temperature. The tetramethylated derivative of parabactin displayed a coalescence temperature of 82 ± 1 °C, which corresponded to an activation energy, E_a, of approximately 19.3 ± 0.2 kcal/mol. The exact coalescence temperature of parabactin's γ-methyl groups was found to be greater than the operating limits of our probe, preventing an accurate measurement of T_c and thus E_a. It was reported earlier that at temperatures around 110 °C, the β-decoupled γ-methyl signal of parabactin could be observed as a single peak.[10] However, closer examination revealed that although the β-decoupled γ-methyl signals of the conformers are merging into one peak, the true coalescence point has not yet been achieved at this temperature. This is evidenced by the unsymmetrical nature of the β-decoupled γ signal. An examination of the nondecoupled spectra of the two γ-methyl doublets better demonstrates this point, where it can be seen that the two γ doublets are not yet completely superimposed on each other at 110 °C. However, the fact that coalescence is beginning at 110 °C allows us to roughly estimate the lower limit of T_c and, hence, E_a of rotation. At 110 °C the peak width at half-height, $\delta\nu$, is 4.5 Hz, which corresponds to an E_a of rotation of 21 kcal/mol. Of course, since E_a varies directly with temperature and inversely with $\delta\nu$, further increases in temperature with concomitant decreases in $\delta\nu$ with lead only to an increase in the value of E_a of rotation. Thus, the estimate of E_a for conformer interconversion of 21 kcal/mol is certainly the lower limit of the true activation energy. The authors wish to emphasize that as only a relative comparison of E_a's was required, total line-shape analysis was not necessary. However, even from this semiquantitative study it is clear that the hydrogen bond donating capacity of the catechol groups plays an important role in conformational isomerism of parabactin.

Amide Protons. In Me_2SO-d_6 the amide protons of the free parabactin overlap in a narrow, complex multiplet between 9.2 and 9.4 ppm, while the NH signals of the parabactin–gallium chelate are considerably more deshielded and appear over a wider

(21) Abraham, P. J.; Perry, K.; Thomas, W. A. *J. Chem. Soc.* **1971**, 446–453.
(22) Peterson, T.; falk, K. T. Leong, S. A.; Klein, M. P.; Neilands, J. B. *J. Am. Chem. Soc.* **1980**, *102*, 7715–7718.
(23) Eng-Wilmot, D. L.; van der Helm, D. *J. Am. Chem. Soc.* **1980**, *102*, 7719–7725.

range between 10.2 and 11.3 ppm. The difference in frequency between the two amide NH signals comprising the major set, 0.26 ppm, and the minor set, 0.78 ppm, both exceed the separation in frequency between amide protons of the free ligand. These observations clearly indicate the parabactin chelate is present as two species, in which a considerable difference in magnetic environments of the amide protons exists between these species.

The extreme downfield shifts experienced by the amide NH protons on going from parabactin to its gallium chelate, up in 1.9 ppm and the fairly large distance between the metal center and amide NHs suggest some phenomenon beyond the metal's charge is contributing to the net deshielding effect of these protons. We wonder if a perturbation occurs in the electronic state of the amide bonds upon metal chelation resulting in a decreased electron density on the amide hydrogens.

The coordination of gallium could result in an electron delocalization in the 2,3-dihydroxybenzamido groups, maximizing conjugation between the aromatic ring and the carbonyl carbon p orbitals. This would decrease the importance of the amide resonance form responsible for maintaining the planarity of the amide linkage, rendering rotation about the C(=O)—N amide bond more feasible. Examination of the various possible structures of the gallium chelate using CPK molecular models indicates a preference for the adoption of a nonplanar amide bond. In this geometry the carbonyl group maintains planarity with the aromatic ring, but ω[24] is significantly altered from its normal angle of 180°. Yan has calculated that the electron density on the amide hydrogen decreases as an amide bond is rotated out of its planar configuration toward 90°.[25] The deshielding of the amide NH protons that would result from such a decrease in electron density might help explain, in part, the large downfield shifts experienced by the amide protons of parabactin on formation of its gallium chelate.

The most striking feature in the ^{1}H NMR spectrum of the parabactin–gallium chelate when observed in D_2O is the presence of only one detectable amide proton signal (Figure 6). The fact that three of the four amide protons are extremely quick to undergo exchange in D_2O while a fourth is so slow to exchange clearly indicates at least one amide NH has limited solvent accessibility. This may be a result of steric shielding, intramolecular hydrogen bonding, or both.

Table I lists the slopes of the chemical shift vs. temperature plot of the four amide NH hydrogens in Me_2SO-d_6. Amide hydrogens that are less accessible to the solvent due to intramolecular hydrogen bonding or are sterically buried display smaller slopes in such plots than amide protons that are able to interact with the solvent.[26-28] All four of the amide NH protons of the parabactin–gallium chelate suggest limited solvent accessibility, as their slopes are smaller than that of *N*-methylacetamide, which showed a slope of 6 (°C/ppm) 10^3. The chemical shift vs. temperature data suggest that, within each of the two sets of amide NH resonances, one of the N–H protons should exchange with the solvent more rapidly than the other. The low-field resonance of the major set exhibits a slope of 0.37 (°C/ppm)10^3 while the high-field peak of the same set exhibits a slope of 0.22. Comparing the slopes of the signals comprising the minor set of NH hydrogens reveals a very large temperature dependence on the chemical shift of the low-field signal of 0.80 (°C/ppm)10^3, indicating a relatively large degree of interaction with the solvent. The high-field peak of the minor set exhibits a slope almost 4 times smaller, 0.18 (°C/ppm)10^3. From the slopes of the chemical shift vs. temperature plot it is apparent that all four of the amide NH hydrogens exhibit restricted interaction with the solvent, with the high-field signal of each set experiencing the least solvent accessibility. The proposal that the high-field amide NH hydrogens experience the greatest restricted interaction with the solvent is confirmed by the addition of a small amount of D_2O to a MeSO-d_6 sample of the parabactin–gallium chelate. All four amide signals persist for several hours with the peaks at 10.78 and 10.33 ppm taking the longest to undergo complete exchange with D_2O.

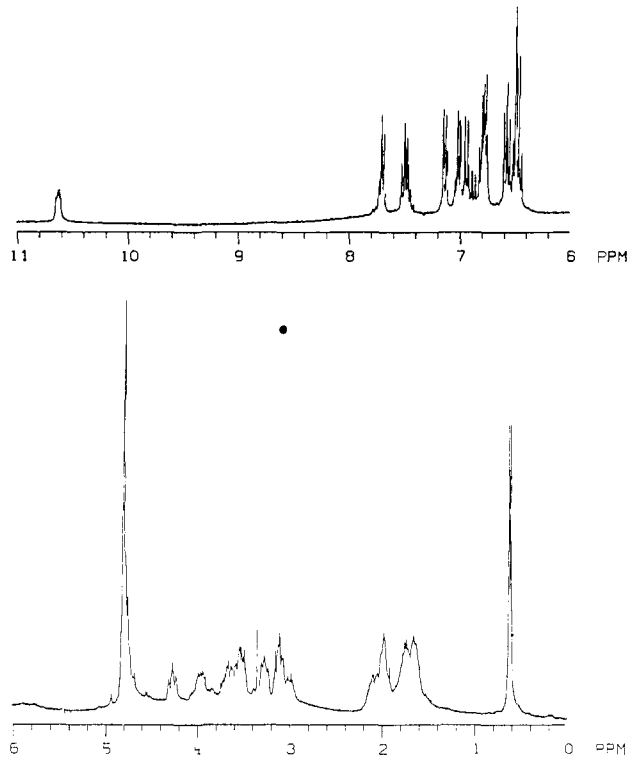

Figure 6. 300-MHz ^{1}H NMR spectrum of the parabactin–gallium(III) chelate in D_2O.

In trying to ascertain whether or not intramolecular hydrogen bonding is responsible for the slow exchange of these amide protons, it is tempting to consider relative chemical shifts of the four amide protons in Me_2SO-d_6. The varying degree of deshielding experienced by the amide protons in MeSO-d_6, evidenced by fairly large differences in their chemical shifts, suggests an approach to determine whether the restricted amide NH interaction with the solvent is a result of intramolecular hydrogen bonding. However, although it is acceptable that intramolecular hydrogen bonding leads to low-field ^{1}H NMR shifts, any attempt at distinguishing the extent of intramolecular hydrogen bonding associated with each amide NH by their relative chemical shifts must be undertaken with extreme caution. Any deshielding contribution to the chemical shift of the amide protons due to intramolecular hydrogen bonding must be considered relative to those amide protons that are hydrogen bonded with the solvent. Since Me_2SO-d_6 is a good hydrogen bond acceptor, hydrogen bonding between the solvent and those protons not involved in intramolecular hydrogen bonds could lead to a greater deshielding of those solvent-exposed protons than protons involved in weak intramolecular hydrogen bonds.[27,29]

External Methylene Protons. From CPK molecular model building it was obvious that the structure of the parabactin–gallium chelate would be rather inflexible, and severe restrictions in the rotation of the methylene units of the spermidine backbone could be expected. This was verified by the gallium chelate's ^{1}H NMR spectrum. The geminal protons on each of the four external carbon atoms of the spermidine backbone, C(1), C(3), C(5), and C(8), all exhibited markedly different chemical shifts (Figure 4). The difference in frequency separating geminal pairs was observed to be greater than 120 Hz for three of the four external methylenes

(24) IUPAC-IUB Commission on Biochemical Nomenclature, *J. Mol. Biol.* **1970**, 1–17.
(25) Yan, L. F.; Momany, F. A.; Hoffmann, R.; Scheraga, H. A. *J. Phys. Chem.* **1970**, *74*, 420.
(26) Ohnishi, M.; Urry, D. W. *Biochem. Biophys. Res. Commun.* **1969**, *36*, 194–202.
(27) Kopple, K. D.; Ohnishi, M.; Go, A. *J. Am. Chem. Soc.* **1969**, *91*, 4264–4272.
(28) Llinās, M.; Klein, M. P.; Neilands, J. B. *J. Mol. Biol.* **1970**, *52*, 399–414.
(29) Kopple, K. D.; Ohnishi, M.; Go, A. *Biochemistry* **1969**, *8*, 4087–4095.

with the largest frequency difference around 360 Hz. This strongly suggests a high degree of rigidity exists in the methylene backbone of the gallium chelate compared to that of the free ligand.

The external methylene protons of the parabactin–gallium chelate are spread out over a larger area than the same external methylene protons of the free ligand in Me_2SO-d_6 or of the pentaanion of parabactin in D_2O. This is an indication that the individual methylene protons in the gallium complex are experiencing substantially different magnetic environments than those of the corresponding protons of the polyanion or free ligand. Upon chelation of gallium, the severe rotational restrictions imposed on the spermidine chain serves to "freeze" the molecules' conformation such that individual geminal protons on each methylene carbon now find themselves in different magnetic environments resulting in different chemical shifts.

If the spermidine chain methylene carbons were free to rotate in the gallium chelate as they are in the free ligand, the chemical shift of the methylene protons would reflect the average of the different magnetic environments experienced by the various rotamers. The chemical shifts of the external methylene protons of the gallium complex in D_2O fall over a 1.3 ppm area between 3.1 and 4.4 ppm, whereas the same protons of the pentaanion fall between 3.3 and 3.8 ppm, over a much smaller area, 0.5 ppm. If one averages the two chemical shift values between each of the four geminal pairs of external methylene protons in the gallium complex in D_2O, the range of these averaged chemical shifts is 3.3–3.7 ppm, almost identical with the range of the methylene protons of the pentaanion in D_2O. In other words, the chemical shifts of geminal pair of protons at 4.3 and 3.1 ppm would average out to 3.7 ppm. Likewise, the geminal pair at 3.5 and 3.1 ppm would average out to 3.3 ppm. The upfield and downfield chemical shifts experienced by geminal protons on the external carbons upon metal chelation could thus be a result of the chelate's relatively "frozen" structure. Such a rigid structure would place the individual methylene protons in shielding or deshielding regions of the adjacent amide groups or adjacent C–C bonds and result in exaggerated chemical shifts between geminal pairs.

The ^1H NMR data of the parabactin–gallium chelate point to inflexibility of the spermidine backbone. The data further suggest that the propyl chain of the spermidine backbone is more restricted to internal C–C rotation than the butyl chain. The difference in frequency between geminal protons on the propyl chain, 360 and 210 Hz, far exceeds the difference between geminal protons on the butyl chain, 120 and 45 Hz. This is consistent with a situation where increased internal C–C rotation by the butyl chain results in an increased averaging of the chemical shifts of the geminal protons. In addition, upon warming a D_2O sample of the parabactin–gallium chelate to 40 °C, the only external methylene signals to undergo a detectable change in chemical shift are the multiplets at 3.55 and 3.60 ppm. These butyl chain protons correspond to the geminal pair on either C(5) or C(8). Additionally, the intramolecular hydrogen bond between the propyl amide proton and the N^4-carbonyl oxygen would certainly be expected to help in freezing the propyl side of the spermidine chain. CPK molecular models clearly show a rigid propyl chain while the butyl methylene chain can undergo a limited amount of internal rotation.

The well-resolved multiplets of the external methylene protons offer an opportunity for the elucidation of dihedral angles between the hydrogens of the spermidine chain via an application of the Karplus equation. In the past few years a number of Karplus curves have been proposed to correlate the angular dependences of the three-bond homonuclear coupling constants $^3J_{NHCH}$ and $^3J_{CHCH}$.[30-32] Establishing a relationship between $^3J_{CHCH}$ and torsional angles is, however, complicated by the fact that ^3J is not only dependent on the dihedral angle between the two protons but also on the electronegativity and orientation of adjacent

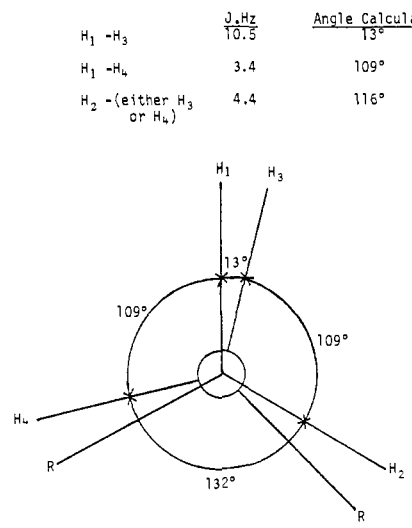

Figure 7. Orientation about the C(3)–C(2) bond suggested by Karplus eq 1.

substituents present in addition to the C–H angles and length of the HC–CH bond.[30] Therefore, attempts at quantitatively relating torsional angles with coupling constants frequently requires a particular treatment for each type of chemical system examined. Notwithstanding these difficulties, three Karplus equations were employed in an attempt to determine the approximate dihedral angles of the propyl chain by $^3J_{NHCH}$ and $^3J_{CHCH}$. The equation used to determine dihedral angles between the propyl chain amide hydrogen and adjacent protons of C(1) was

$$^3J(\theta) = 6.55 \cos^2 \theta - 1.55 \cos \theta + 1.35^{31}$$

while the following equations were used to calculate the CH–CH dihedral angles between protons on C(1)–C(2) and C(3)–C(2)

$$^3J(\theta) = 10.0 \cos^2 \theta - 1.0 \cos \theta + 2.0^{33} \quad (1)$$

$$= 9.4 \cos^2 \theta - 1.4 \cos \theta + 1.6^{34} \quad (2)$$

Throughout the Karplus analysis, referral was made to CPK models to eliminate unlikely choices of θ generated by the equations.

In the elucidation of the orientation of the propyl methylene chain it was found that Karplus eq 1 provided a relatively clear distinction between the possible calculated values of the dihedral angles. These calculated dihedral angles led to an orientation of the propyl methylene chain that was very similar to the orientation suggested by the CPK molecular models.

A combination of the calculated dihedral angles and the orientation of the propyl chain suggested by CPK models enables the assignment of *pro-R* and *pro-S* methylene protons. The validity of the assignment of the absolute configuration at each propyl chain carbon, and thus the Karplus equation used to help elucidate this assignment, can be checked by referring to the double-resonance difference spectral data. This verification can be carried out since the double-resonance difference spectra reveals which of the individual, nonequivalent protons on each of the propyl chain carbons are coupled to, or not coupled to, adjacent protons. It was determined that the assignment of the absolute configuration at each propyl carbon based on Karplus eq 1 did not agree with the results of the double-resonance difference experiments.

For example, Karplus eq 1 and the CPK models suggest the orientation depicted in Figure 7 to exist about the C(3)–C(2) bond. From eq 1, it was determined that proton H_1 (4.26 ppm) is coupled to adjacent H_3 ($J_{H_1H_3}$ = 10.5 Hz, 13°) and to adjacent H_4 ($J_{H_1H_4}$ = 3.4 Hz, 109°). H_2 is coupled to an adjacent proton, H_3 or H_4, with a coupling constant of 4.4 Hz. From eq 1, this coupling constant corresponds to a dihedral angle of 116°. From Figure

(30) Bystrov, V. F. *Prog. Nucl. Magn. Reson. Spectrosc.* **1976**, *10*, 41–81.
(31) Ramachandran, G. N.; Chandrasekaran, R.; Kopple, K. D. *Biopolymers* **1971**, *10*, 2113–2131.
(32) DeMarco, A.; Llinās, M.; Wüthrich, K. *Biopolymers* **1978**, *17*, 617–638.
(33) Hammer, C., personal communication.
(34) Kopple, K. D.; Wiley, G. R.; Tauke, R. *Biopolymers* **1973**, *12*, 627.

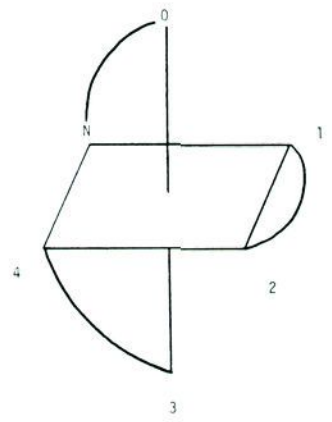

Figure 8. Representation of Λ cis coordination.

7, it can be seen that H_2 must therefore be coupled to H_3. The double-resonance difference spectra show that when H_1 is irradiated, a single large perturbation is observed in the difference spectra in the internal methylene proton region at 2.03 ppm. This large perturbation is, of course, caused by the elimination of a large coupling constant, which corresponds to $J_{H_1H_3}$ = 10.5 Hz. The double-resonance difference spectra also show that irradiation of proton H_2 (3.09 ppm) results in a single perturbation at 1.98 ppm. If the hypothesis that H_2 is coupled to H_3 (as indicated by Karplus eq 1) was correct, then the irradiation of H_2 would have caused a perturbation at 2.03 ppm, not 1.98 ppm.

Because of large errors, eq 2 did not even allow for the distinction between possible calculated values of dihedral angles. Thus, the orientation of the propyl chain using this equation could not be accomplished either. It is clear that neither Karplus eq 1 or 2 is applicable to the propyl chain methylenes of the parabactin–gallium complex. The reason for this is likely related to the role electronegativity plays in coupling.

Discussion

Internals and Double-Resonance Difference Spectroscopy. Double-resonance difference spectroscopy provided the chemical shifts of all six internal methylene protons in addition to revealing which external multiplets are coupled to individual internal resonances (Figure 5). However, the information available from the double-resonance difference spectra is not limited to chemical shift and vicinal coupling information alone but leads directly to the differentiation between those resonances belonging to protons on the propyl chain of the spermidine backbone from those protons on the butyl side.

The separate irradiation of two nongeminal methylene proton multiplets resulting in a single major perturbation at identical chemical shifts in the internal methylene region of their difference spectra can lead to only one conclusion: the two external methylene protons, and the internal methylene proton to which they are both coupled, all lie on the propyl chain of the spermidine backbone. This is exemplified in Table III where it can be seen that irradiation of the two external methylene proton multiplets at 4.26 and 3.27 ppm both produce a single major perturbation in their difference spectra centered at 2.03 ppm. Thus, external protons resonating at 4.26 and 3.27 ppm as well as protons geminal to them, at 3.09 and 3.96 ppm, are all assigned to the protons belonging to the two external methylene carbons of the propyl side of the spermidine chain. Those multiplets located at 3.7, 3.6, 3.55, and 3.14 ppm must all belong to the external protons on the butyl side. Since the lone amide NH proton in D_2O is coupled to protons at 3.96 and 3.27 ppm, this amide NH is therefore on the propyl side of the spermidine backbone. This of course allows the assignment of those multiplets at 3.96 and 3.27 ppm to the geminal protons on C(1) while the peaks at 4.26 and 3.09 ppm must then correspond to the geminal pair on C(3).

Stereochemistry

Because of the unsymmetrical nature of the 2,3-dihydroxybenzoyl groups of parabactin, its gallium chelate can adopt either a cis or trans geometry. Furthermore, two different configurations of the chelating groups about the metal are possible. These are the Λ and Δ optical isomers corresponding to a left- or right-handed "coordination propeller" about the metal atom. From CPK molecular model building it is clear that the *trans*-geometrical coordination isomers are precluded on grounds of steric restraints; however, both of the cis optical isomers Λ and Δ are structurally feasible. The situation is further complicated by the possibility of additional geometrical isomerism arising from the unsymmetrical nature of parabactin's spermidine backbone. Both the Λ and Δ forms can exist in two different geometrical arrangements owing to asymmetry. Figure 8 indicates how two different geometrical isomeric forms can exist for the Λ cis chelate.

In the first form, octahedral coordination positions 1 and 2 are occupied by the catecholate group fixed to the propyl chain of the spermidine backbone, while coordination positions 3 and 4 are occupied by the catecholate moiety attached to the butyl methylene chain. We will refer to this configuration as the Λ cis-3,4 configuration. A second configuration of the Λ cis optical

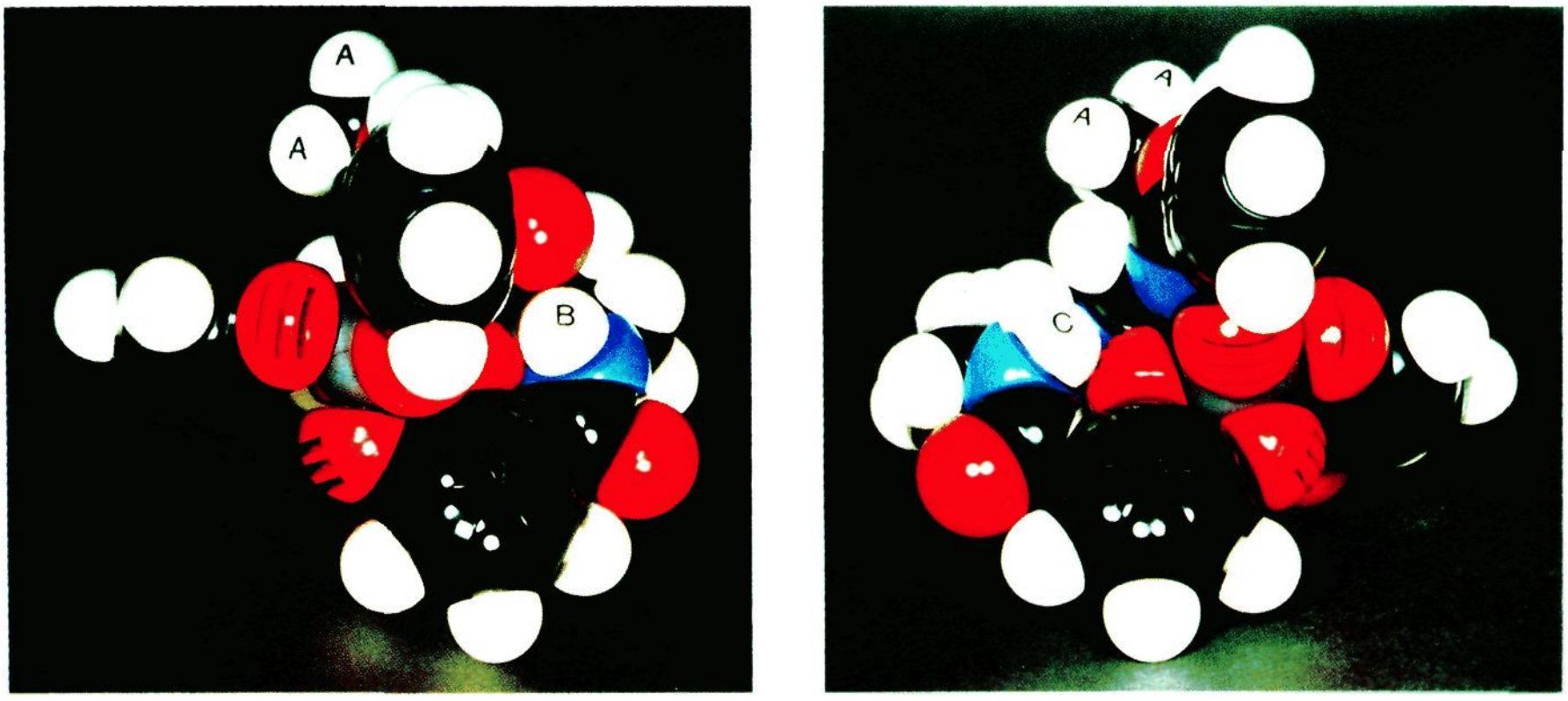

Figure 9. (a, left) CPK model of the parabactin–gallium(III) chelate as the Λ *cis* 3,4-diastereomers. Protons "A" belong to the gamma-methyl group and are positioned in the shielding zone of a nearby aromatic ring. Proton "B" is the propyl amide NH proton. (b, right) CPK model of the parabactin–gallium(III) chelate as the Δ *cis* 3,4-diastereomers. Protons "A" belong to the gamma-methyl group and are not in the shielding zone of any aromatic rings. Proton "C" is the butyl amide NH proton.

isomer exists when coordination positions 1 and 2 are occupied by the catecholate of the butyl chain while the propyl chain catecholate occupies positions 3 and 4, just the opposite orientation of the above. This configuration is referred to as the Λ cis-4,3 configuration. The two geometrical coordination forms of each optical isomer can be envisioned as interconvertible by an approximate 180° rotation of the spermidine backbone about the N^4–CO bond any time prior to the complexation by any two of the three chelating groups in the molecule. An analogous situation, of course, exists for the Δ optical isomer, leading to the formation of two diastereomeric Δ cis coordination isomers.

The asymmetry of ligands possesing chiral carbons can lead to the formation of diastereomeric metal complexes in which one may be formed more favorably than others, or sometimes to the exclusion of all others. Such ligand stereospecificity is exemplified in the case of enterobactin, a catecholamide siderophore whose three L-serine units, which make up its backbone, impart such an asymmetric bias upon chelation that the Δ optical coordination isomer is formed to the exclusion of its Λ diastereomer.[4] From the above, one might expect the formation of the parabactin–metal complex also to result in the preference of one optical coordination isomer over the other. Neilands first obtained evidence to support this by comparing the CD spectrum of parabactin's iron complex with the spectrum of the enterobactin–iron chelate, known to exist as the Δ optical isomer.[7] From the CD spectra of the two metal chelates, Neilands postulated that parabactin exists predominantly in the form of the Λ optical isomer.[7] If Neilands' proposal that the parabactin metal chelate exists predominantly as the Λ optical isomer is correct, one would expect to encounter mainly, if not exclusively, isomers of the Λ cis variety, either the Λ cis-3,4- and/or the Λ cis-4,3 diastereomers. As discussed below, our ^{1}H NMR data are in complete agreement with this expectation.

In Me_2SO-d_6, the γ-methyl signal of parabactin appears as two doublets centered at 1.9 ppm, while the two γ-methyl signals of the parabactin–gallium chelate in the same solvent now occur further upfield at 1.0 ppm. This upfield shift of 0.9 ppm is easily understood after considering the different possible magnetic environments the γ-methyl protons can experience on formation of either Δ cis or Λ cis optical coordination isomers. Inspection of CPK molecular models of the gallium chelate reveals that on formation of the Λ cis optical coordination isomer the γ-methyl group is located directly in the shielding zone of one of the aromatic rings. In fact, both the Λ cis-3,4 and Λ cis-4,3 diastereomers possess a geometry in which the γ-methyl hydrogens are located in the shielding zone of an aromatic ring. Conversely, the γ-methyl group of the Δ cis optical isomer is not in the shielding zone of the aromatic and would not be expected to be deshielded relative to the Λ cis coordination isomer. Therefore, the chemical shift of the γ-methyl protons strongly suggests the chelating groups around the gallium ion adopt the configuration of a left-handed coordination propeller, the Λ form. These findings are in complete agreement with Neilands' initial proposal that the parabactin–iron chelate exists predominantly as the Λ optical isomer. In fact, our studies reveal the Λ optical isomer exists to the exclusion of any Δ coordination isomers. Therefore, the observation of two species in the ^{1}H NMR spectrum of the chelate is not the result of a Λ–Δ isomerization. Instead, the ^{1}H NMR data strongly support the expectation, based on the stereochemical considerations discussed previously, that the gallium chelate exists as a mixture of the two diastereomeric Λ cis coordination isomers.

Inspection of CPK models reveals that intramolecular hydrogen bonding can occur between the N^4-carbonyl oxygen and either the amide NH proton of the propyl chain or the amide NH of the butyl chain in the parabactin–gallium chelate. The question as to how the hydrogen bonding network can be assigned in each of the diastereomers, Λ cis-3,4 or Λ cis-4,3, will now be considered.

It was determined from double-resonance difference spectral studies that the amide NH proton (10.62 ppm, D_2O) most resistant to exchange in D_2O was the NH hydrogen belonging to the propyl chain in the major isomeric species. This proton corresponds to the signal at 10.78 ppm in Me_2SO-d_6. Integration of this proton or its "sister" resonance (11.04 ppm) and the external methylene proton multiplets that are coupled to it indicates that whatever diasteromer they correspond to exists in a 3:1 ratio over the minor isomer. That the "sister" peak (11.04 ppm), which integrates out to the same area as the 10.78 ppm signal, corresponds to the butyl amide proton of the same molecule is further supported by the δ vs. T plots. As expected, the chemical shift of the butyl amide is more sensitive to temperature changes than the propyl amide hydrogen. This is in keeping with its solvent accessibility.

CPK models indicate that if intramolecular hydrogen bonding is the origin of the N–H protons solvent inaccessibility, the major isomer must be the Λ cis-3,4 diastereomer as this is the only low-energy system in which the central amide carbonyl can be hydrogen bonded to the propyl amide hydrogen. Similar considerations indicate that the minor component, the Λ cis-4,3, is so constrained that the butyl amide hydrogen is now hydrogen bonded to the central carbonyl oxygen. The butyl amide hydrogen of the Λ cis-4,3 isomer (10.33 ppm) like the propyl amide hydrogen of the Λ cis-3,4 isomer (10.62 ppm) displays a smaller δ vs. T slope and is much slower to exchange with D_2O in Me_2SO than the corresponding nonintramolecularly hydrogen bonded amide hydrogens.

This analysis results in the assignment of the upfield peaks of each set of amide NH signals as those forming the tightest intramolecular hydrogen bonding. This seems a little strange upon first consideration. However, other factors could be operating in the case of parabactin's gallium chelate, such as deshielding by the solvent of protons able to form intermolecular hydrogen bonds, or, perhaps, differeing degrees of nonplanarity of the terminal amide linkages result in the observed difference in chemical shift of the amide signals. In searching for alternatives one must consider invoking the idea of "sterically burried" protons. Although model building suggests several high-energy conformers would be required to encapsulate the amide protons the final proof awaits an NOE study.

Homochelate, Diastereomer Interconversion, Λ–Δ Racemization. It is proposed that the two sets of signals observed in the ^{1}H NMR spectrum of the parabactin–gallium chelate are due to the presence of two Λ cis coordination diastereomers. Rotation of the spermidine chain about the N^4–CO amide bond prior to the chelation could result in the two diastereomeric chelates. The difference in the orientation of the spermidine chain of the two diastereomeric chelates results in differences in the magnetic environments of the protons of the chelate and hence the presence of duplicate signals. Of course, if the spermidine chain was symmetrical, rotation about the N^4–CO bond prior to chelation would result in two identical conformers, and only one set of NMR signals would be expected. In order to confirm the hypothesis that the duplicate NMR signals are the result of two Λ cis diastereomers, the long symmetrical homologue of parabactin was synthesized, and its gallium chelate was studied. Of course, one has to make the assumption that the long homologue of parabactin will display the same bias in metal chelation that parabactin shows. If the duplicate ^{1}H NMR signals of the parabactin–gallium chelate are indeed the result of two diastereomeric Λ cis coordination isomers, then the ^{1}H NMR spectrum of the long symmetrical chelate will display a single set of peaks. Conversely, if the duplicate ^{1}H NMR signals of the parabactin–gallium chelate are due to a mixture of Λ cis and Δ cis optical isomers, then the long homologue chelate's spectrum would also show duplicate signals.

As expected, the ^{1}H NMR spectrum of the long homologue's gallium chelate, in D_2O and Me_2SO-d_6, shows only one set of resonances. This of course lends further support that the duplicity in parabactin's gallium chelate spectrum is the result of the presence of two Λ cis diastereomers. The observation of the single γ-methyl doublet at an upfield shift of 1.0 ppm, Me_2SO-d_6 is indicative that the long homologue forms the Λ cis coordination isomer. It is interesting that alteration of the backbone chain length by one methylene did not change the preference of the ligand in adopting the Λ optical isomer stereospecifically.

The ^{1}H NMR data strongly suggest the presence of two Λ cis diastereomeric coordination isomers. However, the question of whether they are interconverting remains to be addressed. It seems

unlikely that the two diastereomeric chelates would undergo a rapid rate of interconversion in view of the fact that (1) Ga^{3+} catecholamide complexes typically have high formation constants, on the order of 10^{30}, and (2) the interconversion would require the total dissociation of the two catecholate groups in addition to multiple bond rotations, which would amount to a fairly large expenditure of energy. However, if the two diastereomeric chelates do exist as two rapidly interconverting species, then heating should result in a coalescence of the duplicate signals in the ^1H NMR spectrum.

A sample of the parabactin-gallium chelate in Me_2SO-d_6 was heated over the range 20-130 °C, and although the difference between the two γ-methyl signals decreased with increasing temperature, they never coalesced. In fact, none of the signals present in duplicate in the ^1H NMR spectrum of the chelate coalesced over the temperature range 20-130 °C. The decrease in separation between the two γ-methyl doublets was a result of both signals moving downfield by approximately 20-30 Hz during heating, the upfield doublet moving slightly further downfield than the downfield doublet. It should be pointed out that the γ-methyl signal of the homoparabactin-gallium chelate also displayed a chemical shift dependency on temperature of this same magnitude. Also, after the parabactin-gallium sample was allowed to cool to room temperature after heating to 130 °C, it appeareed identical with that which was taken prior to heating. The data cannot rule out the eventual coalescence between the two diastereomeric coordination isomers. However, the difference between the γ-methyl signals was still 7.3 Hz at 130 °C, which would make the eventual T_c (if one exists) extremely high. It is the belief of the authors that the parabactin-gallium chelate exists as two separate, extremely slow interconverting diastereomers.

An additional point of interest brought out by the ^1H NMR data concerns the rate of racemization of the Λ cis chelate. It is strongly suggested that the Λ cis gallium chelate is formed exclusive of the Δ cis complex. The data also suggest that the Λ cis chelate racemizes to the Δ cis complex very slowly, if at all. Racemization to the Δ chelate would, of course, be easily detected by NMR in the form of additional signals appearing, specifically the appearance of a γ-methyl signal downfield to the γ doublet of the Λ cis chelate. Even after standing in D_2O or Me_2SO-d_6 for several weeks, no additional observable ^1H NMR signals were detected. Additionally, heating a solution of the chelate in Me_2SO-d_6 to 130 °C did not result in any new signals.

Conclusions

The spermidine catecholamide siderophore, parabactin, appears to form a 1:1 complex with gallium(III). The ^1H NMR data strongly suggest the absolute configuration of the parabactin-gallium chelate is Λ cis. Upon complexation with gallium, parabactin appears to form the Λ cis chelate to the exclusion of the Δ cis coordination isomer. Furthermore, the Λ cis gallium complex appears to exist in a 3:1 ratio of two diastereomeric forms, Λ cis-3,4 and Λ cis-4,3 which differ only in the disposition of the spermidine backbone. A ~180° rotation about the N^4-C(O) bond by the ligand any time prior to chelation will lead to the two diastereomeric coordination isomers upon chelation; thus, the conformation equilibrium existing in the free ligand may dictate diastereomer ratios in the metal chelate. This hypothesis lends support to Neilands' proposal that the equilibrium between the two major conformers in the spermidine siderophores results from a cis-trans isomerization about the N^4-C(O) amide bond. Our study further suggests that in the solvents examined, the free ligand, parabactin, exists as three interconverting conformational isomers. Data strongly support the idea that the internal rotational barrier that must be overcome for interconversion of these conformers is partially dependent upon intramolecular hydrogen bonding. In particular, the hydrogen bond donor ability of the catechol groups appears to play a major role in the conformational equilibrium of the ligand.

The elucidation of the stereochemistry of parabactin's gallium chelate will aid in the evaluation of metal-parabactin receptor specificity in *Paracoccus denitrificans*. Experiments are now in progress to evaluate ferric-siderophore outer membrane interactions in various pathogens for the purpose of designing and developing new bacteriostatic agents.

Registry No. 1, 63076-44-8; **2**, 89675-84-3; **3**, 89675-85-4; **4**, 82247-46-9; **5**, 74149-70-5; **6**, 89675-86-5; **7**, 89675-87-6; **8**, 89675-88-7; **9**, 89675-89-8; **10**, 89675-90-1; *N-tert*-butoxycarbonyl-L-threonine, 2592-18-9; N^1,N^8-bis(2,3-dimethoxybenzoyl)spermidine, 78217-75-1; ethyl 2-hydroxybenzimidate, 20857-12-9.

A New NMR Method for Measuring the Difference between Corresponding Proton and Deuterium Chemical Shifts. Isotope Effects on Exchange Equilibria

Martin Saunders,*‡ Susan Saunders, and Constance A. Johnson

Contribution from the Department of Chemistry, Yale University, New Haven, Connecticut 06511. *Received September 2, 1983*

Abstract: A convenient and accurate method is described for measuring the difference between a proton frequency and the corresponding deuterium frequency in its deuterated analogue relative to a reference system by using the deuterium lock in a Fourier-transform NMR spectrometer. This measurement is a sensitive way of measuring equilibrium isotope effects for hydrogen-deuterium exchange. A value of 1.60 per H-D pair is obtained for the equilibrium $2H_3O^+ + 3D_2O \rightleftharpoons 2D_3O^+ + 3H_2O$ at 30 °C in aqueous perchloric acid ($HClO_4$).

Isotope effects on exchange equilibria have previously been measured in several ways as well as calculated from spectroscopic data.[1] Many of the experimental methods are tedious or of limited accuracy, and the spectroscopic data are not always available for the calculations, which are, in addition, time consuming. Since equilibrium isotope effects result from differences in vibrational force constants at sites in different molecules and can yield important information about these variations, it would be desirable

‡ We would like to dedicate this paper to the memory of Susan Saunders who died in January 1982.

(1) For reviews, see: (a) Wolfsberg, M. *Acc. Chem. Res.* **1972**, *5*, 225. (b) Wolfsberg, M. *Annu. Rev. Phys. Chem.* **1969**, *20*, 449.

0002-7863/84/1506-3098$01.50/0 © 1984 American Chemical Society